



Generation of ultracold paraexcitons in cuprous oxide: A path toward a stable Bose-Einstein condensate

Kosuke Yoshioka,¹ Yusuke Morita,¹ Kenta Fukuoka,¹ and Makoto Kuwata-Gonokami^{1,2,*}

¹*Department of Physics, Graduate School of Science, The University of Tokyo, 7-3-1 Hongo, Bunkyo-ku, Tokyo 113-0033, Japan*

²*Photon Science Center, Graduate School of Engineering, The University of Tokyo, 7-3-1 Hongo, Bunkyo-ku, Tokyo 113-8656, Japan*

(Received 29 September 2012; revised manuscript received 25 January 2013; published 23 July 2013)

Cooling of a gas of trapped paraexcitons in Cu₂O to 100 mK, close to the lattice temperature, is reported. We show that the activation of a transverse acoustic scattering mechanism by the applied stress is responsible for the production of ultracold excitons. This low temperature is indispensable to achieving a stable and pure Bose-Einstein condensate of three-dimensional excitons in a strongly inelastic environment.

DOI: [10.1103/PhysRevB.88.041201](https://doi.org/10.1103/PhysRevB.88.041201)

PACS number(s): 67.85.Hj, 63.20.kk, 71.35.Lk

Recent experimental studies of ultracold atoms with controllable interaction strengths have opened up new aspects in many-body quantum physics. They also renewed interest in the search for collective quantum phenomena in photoexcited semiconductors. In particular, in two-dimensional (2D) structures, the research for macroscopic quantum coherence is entering into an active phase, including indirect excitons in coupled quantum well structures and cavity exciton polaritons.^{1–9} Spatial coherence has been confirmed via emitted photons.^{5,6,8–10} Although condensed cavity exciton polaritons are highly nonequilibrium states, they exhibit characteristic properties akin to superfluid phase in liquid helium and atomic BECs, such as quantum vortices^{11–14} and nondiffusive transport.^{15,16} A Berezinskii-Kosterlitz-Thouless-like superfluid phase has also been suggested recently.¹⁷

Such macroscopic quantum phenomena, however, are yet to be investigated in three-dimensional (3D) (bulk) semiconductor systems. Bulk excitons that are weakly coupled to the radiation field are of particular interest and they bear a strong resemblance to hydrogen or positronium atoms. In principle, the long lifetime also allows excitons to reach thermal equilibrium with the crystal lattice temperature through exciton-phonon interactions. The *1s* paraexcitons in cuprous oxide (Cu₂O) provide an example of such excitons that has attracted attention for decades.^{18–27}

An exciton is a photoexcited, bosonic quasiparticle composed of two fermions: an electron and a hole. The possible formation of a Bose-Einstein condensate (BEC) of such elementary excitations in solids attracts much interest both experimentally and theoretically.²⁸ However, BEC of 3D excitons in bulk semiconductors has not yet been directly confirmed since experimental search began about 40 years ago. Much effort has been devoted to observing BEC of *1s* excitons in Cu₂O at superfluid helium temperatures^{18–22,25} ever since the report of quantum degenerate line shapes in phonon-assisted photoluminescence spectra in 1980.²⁹ However, excitonic Lyman spectroscopy in Cu₂O has revealed the emergence of a very large loss mechanism of paraexcitons at increasing densities, which has been attributed to an Auger-like decay process³⁰ similar to that observed in *1s* orthoexcitons.^{31,32} At 2 K, this two-body inelastic collision loss reduces the paraexciton lifetime to the point that it becomes shorter than the characteristic paraexciton-phonon scattering time. This prevents further reduction of the temperature of the dense

exciton gas to that of the lattice. The only possibility for reaching a stable BEC phase is to operate at lower sample temperatures. The conditions for BEC can then be reached at lower exciton densities ($\sim 10^{16}$ cm⁻³) where collision-induced particle loss is largely suppressed.

Recently, by use of a helium-3 refrigerator, a paraexciton gas confined in a potential trap was realized at a temperature of 800 mK, close to the lattice temperature.³³ The critical density for BEC of paraexcitons at 800 mK is 2×10^{16} cm⁻³. As demonstrated recently,^{33,34} when this density was reached at the bottom of the 3D harmonic potential trap, hot excitons suddenly appeared around 0.4 meV above the trap minimum energy. The following explanation for this effect was proposed. The BEC transition is accompanied by a drastic increase in the paraexciton density at the bottom of the trap because of the small volume of the corresponding ground-state wave function. This results in a locally enhanced loss rate due to two-body inelastic scattering and in the sudden appearance of hot excitons at the onset of BEC. This “relaxation explosion” prevents further density increase and thus allows the system to hold only a small condensate fraction; in the case of paraexcitons at a lattice temperature of 800 mK, the maximum estimated condensate fraction is only $\sim 1\%$.

To increase the condensate fraction it is essential to decrease the critical density for BEC even more. This can be obtained by further decreasing the lattice temperature, although it is nontrivial whether the magnitude of the thermal contact between the exciton and phonon systems is sufficient to decrease the exciton temperature at such low temperatures. At an exciton temperature of 100 mK or less, the corresponding critical density is on the order of 10^{14} cm⁻³. The inelastic scattering rate is then reduced by more than an order of magnitude. Further increasing the exciton number dramatically increases the condensate fraction at a density (typically below 10^{16} cm⁻³) where the formed condensate can avoid severe inelastic scattering. Furthermore, by decreasing the trap frequency, which leads to an increase in the volume at the bottom of the trap occupied by the condensate, it is possible to have a spatially large exciton condensate with a larger number of excitons occupying the ground state.

In this Rapid Communication, we show that it is possible to obtain paraexciton temperatures of about 100 mK, which is the lowest temperature ever observed for a gas of 3D excitonic particles with paraexcitons in bulk Cu₂O.^{27,33} This temperature

is far below that normally expected in Cu_2O . Indeed, as discussed below, the main cooling process of paraexcitons freezes out below 1.7 K,³⁵ so the paraexciton temperature should not fall below about 800 mK within a lifetime of several hundred nanoseconds. Here, we show that it is the application of a stress that enables the paraexciton gas to cool to 100 mK.

A cryogen-free dilution refrigerator (Oxford Instruments, DR400) was used in the experiments reported in the present paper. Experiments on paraexcitons in Cu_2O using a dilution refrigerator are also reported in Ref. 27. A high-purity, natural single crystal of Cu_2O ($5.3 \times 5.3 \times 8.0$ mm) was attached to the mixing chamber with great care in order to maximize thermal conductivity from the sample to the mixing chamber. In addition, we attached two piezoelectric stages on the mixing chamber: one stage to apply variable stress (up to 2.7 kbar in the present experiment) to the sample crystal, and the other to adjust the position of the lens (focal length $f = 15$ mm) collecting the weak luminescence from trapped paraexcitons. The details of the setup will be described elsewhere. The collected luminescence light was collimated and sent outside the refrigerator through antireflection-coated windows that act as radiation shields. A fivefold magnified image of the trapped paraexciton gas was formed on the entrance slit of a 50 cm imaging spectrometer with an electron-multiplying charge coupled device attached. This allows us to acquire spatially resolved luminescence spectra of paraexcitons with spatial and spectral resolution of $10 \mu\text{m}$ and $60 \mu\text{eV}$, respectively. To improve the spectral resolution further, the collimated light passed through a solid etalon ($R = 90\%$, $\text{FSR} = 648 \mu\text{eV}$). By acquiring a series of spatially resolved spectra by tilting the angle of the solid etalon, we can reconstruct a high-resolution, spatially resolved spectrum. The spectral resolution is $22 \mu\text{eV}$ in full width at half maximum. The excitation configuration is identical to that of our previous experiments using a ^3He refrigerator.^{33,34} Creation of $1s$ orthoexcitons was accomplished via a longitudinal-optical phonon-assisted absorption process under illumination of a continuous-wave (cw) light at 606 nm. The generated orthoexcitons converted into paraexcitons and the paraexcitons were trapped and accumulated in the trap potential. To preclude any heating effect, the incident power was set to 3 nW.

Figure 1(a) shows a typical result taken at $T_L = 40$ mK (T_L is the lattice temperature). The maximum applied stress was 1.4 kbar, and the geometric mean of the trap frequencies

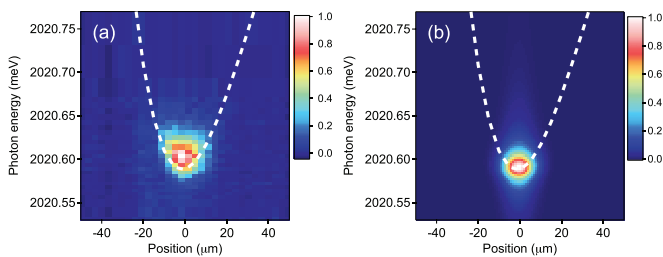


FIG. 1. (Color online) (a) Typical spatially resolved luminescence spectrum at $T_L = 40$ mK. The excitation power is 3 nW. The dotted curve indicates the trap potential. (b) Calculated spatially resolved spectrum assuming $T_{ex} = 150$ mK. This temperature best reproduces the spectral and spatial width of the figure on the left. T_L and T_{ex} are the lattice and the exciton temperature, respectively.

was 23 MHz. The applied stress was determined from the maximum energy shift of the paraexciton level in the trap. We performed a numerical simulation to reproduce the spatially resolved spectrum for any specified temperature, taking into account our experimental resolution and the stress-dependent strength of the direct luminescence process when paraexcitons recombine. The simulation reproduced well the spatial and spectral broadening when the paraexciton temperature was set to 150 mK [Fig. 1(b)].

As mentioned before, this exciton temperature is unexpectedly low when considering the paraexciton lifetime. The lowest possible paraexciton temperature is determined by the exciton-phonon interaction rate and the lifetime of paraexcitons. It is well known that exciton cooling proceeds mainly via phonon emission. Only longitudinal acoustic (LA) phonons are allowed to interact at low temperature with paraexcitons in a strain-free environment on account of symmetry requirements. The rate of cooling by this process drastically decreases below a characteristic temperature that is determined by the linear dispersion of acoustic phonons and the parabolic dispersion of the center-of-mass motion of excitons. This is because the phonon emission process cannot reach a final exciton state while satisfying the momentum and energy conservation rules [see Fig. 2(a)]. The characteristic temperature for this “freezing out” of the LA phonon emission is 1.7 K, taking into account the velocity of LA phonons (4.5 km/s) and the effective mass of paraexcitons ($2.6m_0$; m_0 is the free electron mass at rest).^{36,37} The measured lifetime of trapped paraexcitons at low densities in our sample is 300 ns. In this case, calculations indicate that the lowest paraexciton temperature should be about 800–900 mK. Indeed, the measured temperature of untrapped paraexcitons is 710 mK at a lattice temperature of 56 mK.

The deviation between the actual paraexciton temperature in a trap and the expected temperature indicates the presence of a new cooling channel for paraexcitons. We attribute this

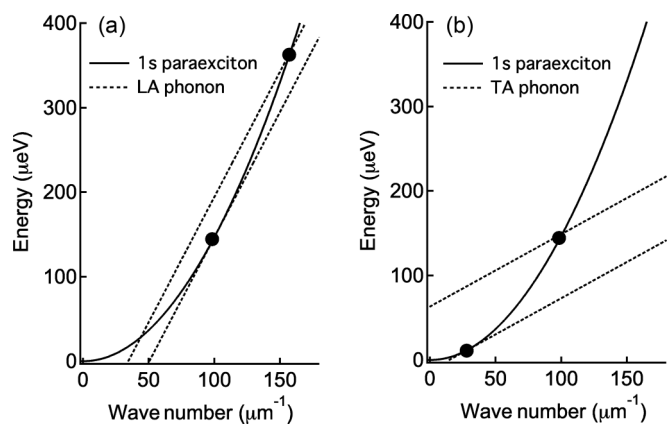


FIG. 2. Energy and momentum conservation in the cooling process of $1s$ paraexcitons via acoustic phonon emission. (a) Solid curve shows the dispersion relation of the $1s$ paraexciton state and the dashed lines show the LA phonon dispersion relations. Paraexcitons having the kinetic energies of less than $150 \mu\text{eV}$ [$k_B \times (1.7 \text{ K})$] can emit no LA phonons. (b) Because of the slower velocity of TA phonons (dashed line), such a limiting kinetic energy reduces to $12.5 \mu\text{eV}$ [$k_B \times (145 \text{ mK})$].

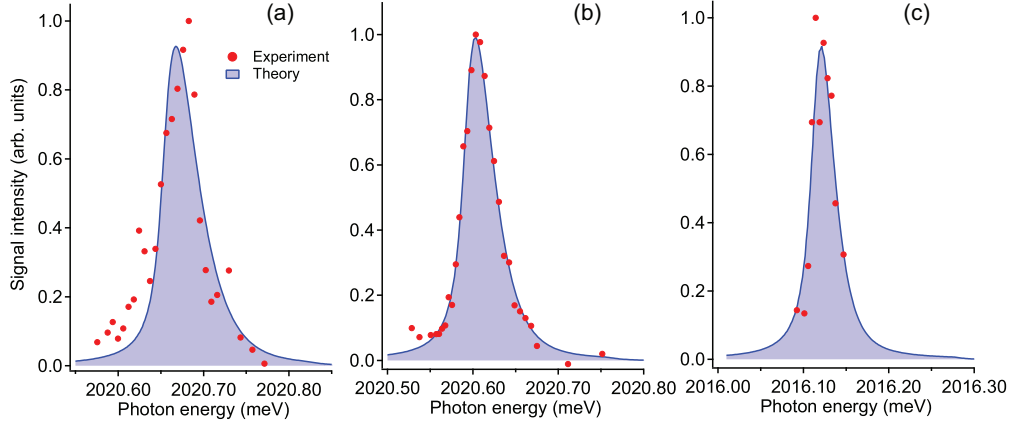


FIG. 3. (Color online) Luminescence spectra of trapped paraexcitons at $T_L = 40$ mK. The photons are emitted directly when paraexcitons recombine radiatively under a strain field, a rare occurrence. (a) The paraexciton temperature is $T_{ex} = 207 \pm 37$ mK under an applied stress of 1.0 kbar. (b) $T_{ex} = 159 \pm 7$ mK at 1.4 kbar. (c) $T_{ex} = 97 \pm 33$ mK at 2.7 kbar.

channel to the interaction between paraexcitons and transverse acoustic (TA) phonons, an interaction that is allowable under a strain field because of the lowering of the crystal symmetry. The velocity of TA phonons is about one-third of that of LA phonons, allowing paraexcitons to be cooled to much lower temperatures [see Fig. 2(b)]. The same activation mechanism was proposed to explain the temperature dependence of the mobility of paraexcitons under an applied stress.³⁵ Our interpretation is based on the following evidence: (1) the lowest paraexciton temperature is stress dependent and (2) the lowest paraexciton temperatures systematically coincide with numerical simulation based on the Boltzmann equations.

Figure 3 shows the luminescence spectra of the direct emission from the trapped paraexcitons, taken under the different trap potentials formed. The lattice temperature is 40 mK for all cases. The measured paraexciton temperature is clearly dependent on the applied stress. Specifically, the exciton temperature is $T_{ex} = 207 \pm 37$ mK at an applied stress of $\sigma = 1.0$ kbar [Fig. 3(a)], $T_{ex} = 159 \pm 7$ mK at $\sigma = 1.4$ kbar [Fig. 3(b), identical data to Fig. 1], and $T_{ex} = 97 \pm 33$ mK at $\sigma = 2.7$ kbar [Fig. 3(c)]. The paraexciton temperature is greatly reduced to near lattice temperature in the presence of the finite strain field. These data were recorded with different combinations of radius of curvature of the stressor and applied force, using the same sample. Therefore, the results directly reflect the dependence of the paraexciton temperature on applied stress.

To understand the stress-dependent reduction of the temperature of dilute paraexcitons, here we numerically estimate the lowest possible paraexciton temperature by taking into account the possible interaction between paraexcitons and TA phonons, as well as LA phonons. The numerical simulation utilizes the following conventional Boltzmann equation:

$$\begin{aligned} \frac{dN_{\vec{k}}}{dt} = & -\frac{2\pi}{\hbar} \sum_q \frac{\hbar \Xi_{LA}^2 q}{2V\rho v_{LA}} \{ [(1 + N_{\vec{q}}^{LA})(1 + N_{\vec{k}-\vec{q}})N_{\vec{k}} \\ & - N_{\vec{q}}^{LA}N_{\vec{k}-\vec{q}}(1 + N_{\vec{k}})] \delta(E_{\vec{k}} - E_{\vec{k}-\vec{q}} - \hbar\omega_{\vec{q}}^{LA}) \\ & + [N_{\vec{q}}^{LA}(1 + N_{\vec{k}+\vec{q}})N_{\vec{k}} - (1 + N_{\vec{q}}^{LA})N_{\vec{k}+\vec{q}}(1 + N_{\vec{k}})] \\ & \times \delta(E_{\vec{k}} - E_{\vec{k}+\vec{q}} + \hbar\omega_{\vec{q}}^{LA}) \} \end{aligned}$$

$$\begin{aligned} -\frac{2\pi}{\hbar} \sum_q \frac{\hbar \Xi_{TA}^2 q}{2V\rho v_{TA}} \{ [(1 + N_{\vec{q}}^{TA})(1 + N_{\vec{k}-\vec{q}})N_{\vec{k}} \\ - N_{\vec{q}}^{TA}N_{\vec{k}-\vec{q}}(1 + N_{\vec{k}})] \delta(E_{\vec{k}} - E_{\vec{k}-\vec{q}} - \hbar\omega_{\vec{q}}^{TA}) \\ + [N_{\vec{q}}^{TA}(1 + N_{\vec{k}+\vec{q}})N_{\vec{k}} - (1 + N_{\vec{q}}^{TA})N_{\vec{k}+\vec{q}}(1 + N_{\vec{k}})] \\ \times \delta(E_{\vec{k}} - E_{\vec{k}+\vec{q}} + \hbar\omega_{\vec{q}}^{TA}) \}, \end{aligned} \quad (1)$$

where \vec{q} , $\rho = 6.1$ g/cm³, and V are the phonon wave vector, crystal density of Cu₂O, and crystal volume, respectively. $N_{\vec{q}}^{LA}$ and $N_{\vec{q}}^{TA}$ are the numbers of LA and TA phonons at \vec{q} . $N_{\vec{k}}$ is the number of excitons having the wave vector \vec{k} . Ξ_{LA} is the effective deformation potential that determines the interaction strength between paraexcitons and LA phonons. Here we set $\Xi_{LA} = 1.68$ eV.³⁸ The velocity of the LA phonons is $v_{LA} = 4.5 \times 10^3$ m/s.³⁵ The effective deformation potential between paraexcitons and TA phonons is proportional to the applied stress σ , since the shear strain contribution on the paraexciton energy has a quadratic dependence on the applied static stress. Here we set a positive parameter α , which is the ratio between the effective deformation potentials,

$$\frac{\Xi_{TA}}{\Xi_{LA}} = -\alpha\sigma, \quad (2)$$

and use this Ξ_{TA} in the calculation. The TA phonon velocity v_{TA} is 1.3×10^3 m/s.³⁵ The measured lifetime of paraexcitons is 300 ns. We calculate the minimum paraexciton temperature under a weak cw excitation condition with α as the only adjustable parameter. Note that we neglect the angle dependence of the TA phonon scattering with respect to the axis of the applied stress, considering our system to be in a steady state and such a dependence is averaged. In addition, we neglect the contribution of the shear strain component in the deformation potential on paraexciton-LA-phonon scattering, which also becomes effective under an applied stress. This is because the LA phonons contribute only negligibly in the temperature range of interest (< 800 mK) as discussed above.

Figures 4(a)–4(c) show the calculated applied stress dependence of the lowest paraexciton temperature at $T_L = 40$ mK. The curves are well fitted with the Maxwell-Boltzmann

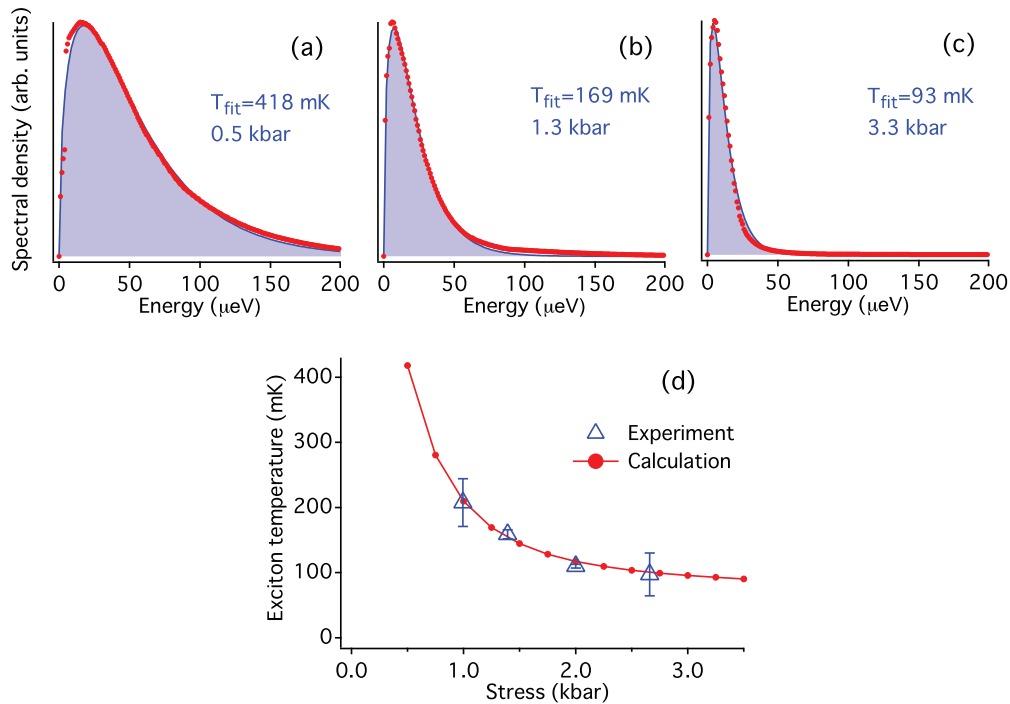


FIG. 4. (Color online) (a)–(c) Calculated stress dependence of the thermal distribution of paraexcitons at 300 ns (filled circles). α (see text) is set to 0.2 kbar^{-1} . (Blue curves with shading) Fitted curves using the Maxwell-Boltzmann distribution function. (d) Extracted stress dependence of the calculated paraexciton temperature at 300 ns (filled circles) and experimental data (open triangles, extracted from Fig. 3). The experimental spectrum at 2.0 kbar is not shown in Fig. 3.

distribution function shown in each figure. The lowest paraexciton temperature decreases drastically as the applied stress is increased and even approaches the temperature of the crystal lattice. The calculated stress dependence for the lowest temperature ($\alpha = 0.2 \text{ kbar}^{-1}$) and the actual paraexciton temperature under several conditions is plotted in Fig. 4(d). We can find perfect coincidence between the calculated and experimental data.

From the facts discussed above, we conclude that the application of stress brings about finite paraexciton-TA-phonon interactions that are essential for paraexcitons to reach the 100 mK region or below within their limited lifetimes. This means that the phonon bath can be used as a coolant for paraexcitons at sub-Kelvin temperatures. This finding is of particular importance to realize a collision-free, ideal, quantum-mechanical gas whose thermal distribution is determined by perfect thermal contact with a thermal bath, not by thermal redistribution through elastic collisions between constituent particles as in atomic BECs. Suppose that we reach the BEC phase boundary at a critical temperature in the sub-Kelvin region. For ideal bosons, further increasing the exciton number in the trap by a factor of 10 while keeping the exciton temperature constant, results in a condensate fraction of 90%. However, in the present system the frequent inelastic scattering at high density suppresses the condensate fraction by shortening the exciton lifetime and possibly heating the system. Thus, it is vital to realize a BEC transition at the lowest density possible, from $2 \times 10^{16} \text{ cm}^{-3}$ at 800 mK to possibly $2 \times 10^{14} \text{ cm}^{-3}$ at 40 mK, by cooling the paraexciton gas through the mechanism discussed in the present paper.

Elucidating the physical origin of the inelastic scattering process will allow us to rigorously study the stability of the Bose-Einstein condensation of this system. Determining the amount of excess energy per collision, which is completely unknown, is especially important.

In conclusion, we have found that trapped paraexcitons in cuprous oxide can be cooled to 100 mK by the activation of interactions between paraexcitons and transverse acoustic phonons under the application of a stress. Without applied stress, the paraexciton temperature could not cool below 800 mK within a lifetime of 300 ns because the paraexciton-LA-phonon interactions freeze-out at sub-Kelvin temperatures. To obtain a large stable fraction of cold Bose-condensed paraexcitons in Cu_2O , it is necessary to apply a strong stress that efficiently cools the gas and also to prepare a modest trap potential having a low trap frequency so as to reduce two-body collision-induced losses. The activation of this cooling channel is also important for preparing and cooling relatively high-density gases of paraexcitons with which to study nonlinear phenomena once the dilute BEC is confirmed.

We thank A. Mysyrowicz for valuable discussions and critically reading the manuscript. This work was supported by a Grant-in-Aid for Scientific Research on Innovative Area “Optical science of dynamically correlated electrons (DYCE)” 20104002 and the Photon Frontier Network Program of the Ministry of Education, Culture, Sports, Science and Technology, Japan, and by JSPS through its FIRST Program.

*gonokami@phys.s.u-tokyo.ac.jp

- ¹R. M. Stevenson, V. N. Astratov, M. S. Skolnick, D. M. Whittaker, M. Emam-Ismael, A. I. Tartakovskii, P. G. Savvidis, J. J. Baumberg, and J. S. Roberts, *Phys. Rev. Lett.* **85**, 3680 (2000).
- ²J. J. Baumberg, P. G. Savvidis, R. M. Stevenson, A. I. Tartakovskii, M. S. Skolnick, D. M. Whittaker, and J. S. Roberts, *Phys. Rev. B* **62**, R16247 (2000).
- ³H. Deng, G. Weihs, C. Santori, J. Bloch, and Y. Yamamoto, *Science* **298**, 199 (2002).
- ⁴L. V. Butov, A. C. Gossard, and D. S. Chemla, *Nature (London)* **418**, 751 (2002).
- ⁵A. Baas, J. P. Karr, M. Romanelli, A. Bramati, and E. Giacobino, *Phys. Rev. Lett.* **96**, 176401 (2006).
- ⁶J. Kasprzak, M. Richard, S. Kundermann, A. Baas, P. Jeambrun, J. M. J. Keeling, F. M. Marchetti, M. H. Szymańska, R. André, J. L. Staehli *et al.*, *Nature (London)* **443**, 409 (2006).
- ⁷R. Balili, V. Hartwell, D. W. Snoke, L. Pfeiffer, and K. West, *Science* **316**, 1007 (2007).
- ⁸A. A. High, J. R. Leonard, A. T. Hammack, M. M. Fogler, L. V. Butov, A. V. Kavokin, K. L. Campman, and A. C. Gossard, *Nature (London)* **483**, 584 (2012).
- ⁹A. A. High, J. R. Leonard, M. Remeika, L. V. Butov, M. Hanson, and A. C. Gossard, *Nano Lett.* **12**, 2605 (2012).
- ¹⁰H. Deng, G. S. Solomon, R. Hey, K. H. Ploog, and Y. Yamamoto, *Phys. Rev. Lett.* **99**, 126403 (2007).
- ¹¹K. G. Lagoudakis, M. Wouters, M. Richard, A. Baas, I. Carusotto, R. André, L. S. Dang, and B. Deveaud-Pledran, *Nat. Phys.* **4**, 706 (2008).
- ¹²K. G. Lagoudakis, T. Ostatnický, A. V. Kavokin, Y. G. Rubo, R. André, and B. Deveaud-Pledran, *Science* **326**, 974 (2009).
- ¹³D. Sanvitto, F. M. Marchetti, M. H. Szymanska, G. Tosi, M. Baudisch, F. P. Laussy, D. N. Krizhanovskii, M. S. Skolnick, L. Marrucci, A. Lemaitre *et al.*, *Nat. Phys.* **6**, 527 (2010).
- ¹⁴G. Roumpos, M. D. Fraser, A. Löffler, S. Höfling, A. Forchel, and Y. Yamamoto, *Nat. Phys.* **7**, 129 (2010).
- ¹⁵A. Amo, D. Sanvitto, F. P. Laussy, D. Ballarini, E. D. Valle, M. D. Martin, A. Lemaître, J. Bloch, D. N. Krizhanovskii, M. S. Skolnick *et al.*, *Nature (London)* **457**, 291 (2009).
- ¹⁶A. Amo, J. Lefrère, S. Pigeon, C. Adrados, C. Ciuti, I. Carusotto, R. Houdré, E. Giacobino, and A. Bramati, *Nat. Phys.* **5**, 805 (2009).
- ¹⁷G. Roumpos, M. Lohse, W. H. Nitsche, J. Keeling, M. H. Szymanska, P. B. Littlewood, A. Löffler, S. Höfling, L. Worschech, A. Forchel *et al.*, *Proc. Natl. Acad. Sci. USA* **109**, 6467 (2012).
- ¹⁸D. P. Trauernicht, J. P. Wolfe, and A. Mysyrowicz, *Phys. Rev. B* **34**, 2561 (1986).
- ¹⁹D. W. Snoke, J. P. Wolfe, and A. Mysyrowicz, *Phys. Rev. B* **41**, 11171 (1990).
- ²⁰D. W. Snoke, J. L. Lin, and J. P. Wolfe, *Phys. Rev. B* **43**, 1226 (1991).
- ²¹J. L. Lin and J. P. Wolfe, *Phys. Rev. Lett.* **71**, 1222 (1993).
- ²²E. Fortin, S. Fafard, and A. Mysyrowicz, *Phys. Rev. Lett.* **70**, 3951 (1993).
- ²³H. Shi, G. Verechaka, and A. Griffin, *Phys. Rev. B* **50**, 1119 (1994).
- ²⁴L. Bányai, P. Gartner, O. M. Schmitt, and H. Haug, *Phys. Rev. B* **61**, 8823 (2000).
- ²⁵N. Naka and N. Nagasawa, *Solid State Commun.* **126**, 523 (2003).
- ²⁶C. Sandfort, J. Brandt, C. Finke, D. Fröhlich, M. Bayer, H. Stolz, and N. Naka, *Phys. Rev. B* **84**, 165215 (2011).
- ²⁷R. Schwartz, N. Naka, F. Kieseling, and H. Stolz, *New J. Phys.* **14**, 023054 (2012).
- ²⁸S. A. Moskalenko and D. W. Snoke, *Bose-Einstein Condensation of Excitons and Biexcitons* (Cambridge University Press, Cambridge, UK, 2000).
- ²⁹D. Hulin, A. Mysyrowicz, and C. Benoît à la Guillaume, *Phys. Rev. Lett.* **45**, 1970 (1980).
- ³⁰K. Yoshioka, T. Ideguchi, A. Mysyrowicz, and M. Kuwata-Gonokami, *Phys. Rev. B* **82**, 041201(R) (2010).
- ³¹K. E. O'Hara and J. P. Wolfe, *Phys. Rev. B* **62**, 12909 (2000).
- ³²D. W. Snoke and V. Negoita, *Phys. Rev. B* **61**, 2904 (2000).
- ³³K. Yoshioka, E. Chae, and M. Kuwata-Gonokami, *Nat. Commun.* **2**, 328 (2011).
- ³⁴K. Yoshioka and M. Kuwata-Gonokami, *New J. Phys.* **14**, 055024 (2012).
- ³⁵D. P. Trauernicht and J. P. Wolfe, *Phys. Rev. B* **33**, 8506 (1986).
- ³⁶J. Brandt, D. Fröhlich, C. Sandfort, M. Bayer, H. Stolz, and N. Naka, *Phys. Rev. Lett.* **99**, 217403 (2007).
- ³⁷K. Yoshioka, T. Ideguchi, and M. Kuwata-Gonokami, *Phys. Rev. B* **76**, 033204 (2007).
- ³⁸K. Reimann and K. Syassen, *Phys. Rev. B* **39**, 11113 (1989).